Magnetic Anisotropies in Rhombic Lanthanide(III) Complexes Do Not Conform to Bleaney's Theory

Goretti Castro[a], Martín Regueiro-Figueroa[b], David Esteban-Gómez[b], Paulo Pérez-Lourido[a], Carlos Platas-Iglesias[*b], and Laura Valencia[a]

[a] Departamento de Química Inorgánica, Facultad de Ciencias, Universidade de Vigo, As Lagoas, Pontevedra, Marcosende 36310, Spain

[b] Centro de Investigaciones Científicas Avanzadas (CICA) and Departamento de Química Fundamental, Universidade da Coruña, Campus da Zapateira-Rúa da Fraga 10, 15008 A Coruña, Spain

Inorganic Chemistry Volume 55, Issue 7, pages 3490–3497, April 4, 2016
Received: 21 December 2015, Published online: 15 March 2016, Published in print: 4 April 2016

How to cite:

Magnetic Anisotropies in Rhombic Lanthanide(III) Complexes Do Not Conform to Bleaney's Theory. Goretti Castro, Martín Regueiro-Figueroa, David Esteban-Gómez, Paulo Pérez-Lourido, Carlos Platas-Iglesias, and Laura Valencia. *Inorganic Chemistry* **2016** *55* (7), 3490-3497. DOI: 10.1021/acs.inorgchem.5b02918

Abstract

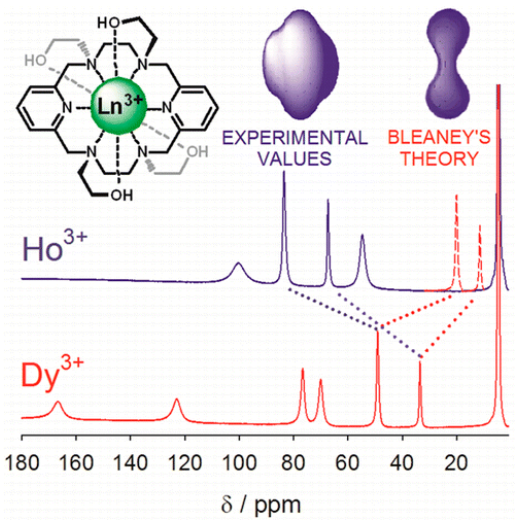

We report a complete set of magnetic susceptibilities of lanthanide complexes with a macrocyclic ligand based on a 3,6,10,13-tetraaza-1,8(2,6)-dipyridinacyclotetradecaphane platform containing four hydroxyethyl pendant arms (L^1). The $[LnL^1]^{3+}$ complexes are isostructural along the lanthanide series from Ce^{3+} to Yb^{3+}, with the only structural change observed along the series being the monotonous shortening of the Ln–donor distances due to lanthanide contraction. The ^1H NMR spectra point to a D_2 symmetry of the $[LnL^1]^{3+}$ complexes in aqueous solution, which provides a unique opportunity for analysis of the rhombic magnetic anisotropies with an unequivocal location of the magnetic axes. The contact contributions for the observed paramagnetic shifts have been estimated with density functional theory calculations on the $[GdL^1]^{3+}$ complex. Subsequently, the pseudocontact shifts could be factored out, thereby giving access to the axial and rhombic contributions of the magnetic susceptibility tensor. Our results show that the calculated magnetic anisotropies do not follow the trends predicted by Bleaney's theory, particularly in the case of Ho^{3+} and Er^{3+} complexes.

Keywords: contrast agents; coordination compounds; gadolinium; lanthanides; NMR imaging

Introduction

The paramagnetic properties of trivalent lanthanide ions (Ln^{3+}) have been exploited in NMR for more than 4 decades. Complexes of the Ln^{3+} ions were widely used as shift reagents in the early times of NMR to reduce the complexity of second-order NMR spectra[1] because the use of an appropriate paramagnetic shift reagent induces significant chemical shifts without provoking excessive line broadening.[2] Shift reagents were particularly useful before high-field NMR spectrometers became routinely available. Later, chiral shift reagents were introduced in the analysis of mixtures of enantiomers and the assignment of an absolute configuration,[3] an application that continues to be important nowadays.[4] The paramagnetic shifts induced by Ln^{3+}were also intensively used for the determination of the structure and conformational properties of flexible molecules[5] and proteins[6] and of intra- and extracellular Na^{+}.[7]

The paramagnetic properties of Gd^{3+} associated with its ^{8}S electronic ground state make this metal ion an ideal candidate for the preparation of contrast agents in magnetic resonance imaging.[8] However, contrast agents based on the chemical exchange saturation transfer (CEST) approach represent an attractive alternative to the classical Gd^{3+}-based agents.[9] CEST agents contain a pool of exchangeable protons in intermediate-to-slow condition with bulk water ($k_{ex} \leq \Delta\omega$). Application of a presaturation pulse at the frequency of the exchangeable protons transfers some saturated spins into the water pool, which attenuates the signal of bulk water.[9,10] Complexes of paramagnetic Ln^{3+} ions shift the resonance of the exchanging protons well away from the bulk water resonance, so that the exchange rate of the exchangeable protons (k_{ex}) can be faster while keeping the slow-to-intermediate exchange regime.[10] A similar approach was used to generate the CEST effect by loading liposomes with paramagnetic Ln^{3+} complexes that shift the resonance of water molecules inside the liposome.[11] Similarly, paramagnetic Ln^{3+}complexes have been used as chemical shift imaging reagents in vivo.[12]

The NMR signals due to ligand nuclei in paramagnetic Ln^{3+} complexes experience large frequency shifts as a result of both contact (δ_{ij}^{con}) and pseudocontact (δ_{ij}^{pscon}) contributions:[13]

$$\delta_{\mathrm{ij}}^{\mathrm{para}} = \delta_{ij}^{\mathrm{exp}} - \delta_{i}^{\mathrm{dia}} = \delta_{ij}^{\mathrm{con}} + \delta_{ij}^{\mathrm{pscon}} \qquad (1)$$

where δ_{ij}^{para} represents the paramagnetic shift induced by a lanthanide ion *j* in a nucleus *i* and δ_{i}^{dia} accounts for the diamagnetic contribution. The pseudocontact contribution results from the local magnetic field induced in the nucleus under study by the magnetic moment of the Ln^{3+} ion and can be written as in eq 2 if the reference frame coincides with the main directions of the magnetic susceptibility tensor χ:[13,14]

$$\delta_{ij}^{\mathrm{pscon}} = \frac{1}{12\pi r^{3}}\left[\Delta\chi_{\mathrm{ax}}\left(\frac{3z^{2}-r^{2}}{r^{2}}\right) + \frac{3}{2}\Delta\chi_{\mathrm{rh}}\left(\frac{x^{2}-y^{2}}{r^{2}}\right)\right] \qquad (2)$$

where $r = \sqrt{x^2 + y^2 + z^2}$, in which *x*, *y*, and *z* are the Cartesian coordinates of a nucleus *i* relative to the location of a Ln^{3+} ion *j* placed at the origin, and $\Delta\chi_{ax}$ and $\Delta\chi_{rh}$ are the axial and rhombic parameters of the symmetric magnetic susceptibility tensor. For the special case of axial symmetry, which holds for systems containing a C_n axis with $n \geq 3$, $D_2 = 0$. Bleaney[15] proposed back in 1972 that the magnetic susceptibility tensor can be approximated in a power series of the inverse temperature. The first term in T^{-1} described the isotropic magnetic susceptibility $\chi_0 = 1/3Tr$, while the terms in T^{-2} correspond to the anisotropic part of the

magnetic susceptibility, which Bleaney related to the conventional B_0^2 and B_2^2 crystal-field parameters of the second degree:

$$\delta_{ij}^{\mathrm{pscon}} = C_j B_0^2 \left(\frac{3z^2-r^2}{r^5}\right) + \sqrt{6} C_j B_2^2 \left(\frac{x^2-y^2}{r^5}\right) \qquad (3)$$

Here, C_j are the so-called Bleaney factors,[15] which are calculated as[16,17]

$$C_j = \frac{-N_A \beta^2 (1+p_j) \xi_j}{60(kT)^2} \qquad (4)$$

where ξ_j is a numerical factor characteristic of each $4f^n$ configuration and $1 + p_j$ accounts for thermally populated excited states. Bleaney assumed that the energy of the crystal-field splitting created by the crystal-field parameters B_0^2 and B_2^2 is much smaller than kT, so that all crystal-field levels of the ground state possess similar populations. The validity of Bleaney's theory has been the subject of some debate. Deviations of pseudocontact shift patterns from Bleaney's theory have often been attributed to variations of the crystal-field parameters across the lanthanide series.[18] Indeed, Binnemans and co-workers showed that Bleaney's approach does not provide a good quantitative approximation because it limits the temperature expansion of the magnetic susceptibility in the inverse temperature to T^{-2} terms.[19] More recently, the validity of the point electron-dipole approximation was also put into question.[20] In a recent paper, Parker and co-workers have also shown that the pseudocontact shifts of axially symmetric Ln^{3+}complexes do not follow the trend expected from the respective C_j values.[21] However, Bertini and co-workers found that Bleaney's theory is in excellent qualitative agreement with the magnetic anisotropies obtained for the dicalcium protein D_{9k} incorporating the full series of Ln^{3+} ions into the C-terminal calcium binding site.[22]

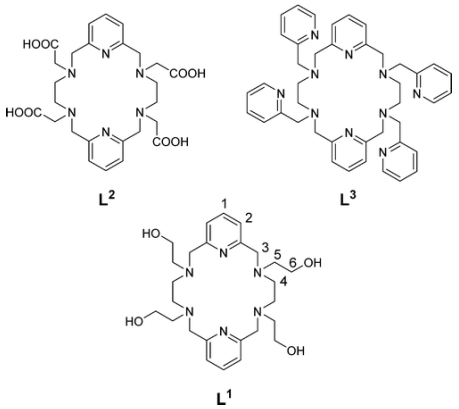

Chart 1. Ligands Discussed in the Present Work and the Numbering Scheme Used for NMR Spectral Assignment of the Complexes of L^1

The magnetic anisotropy of Ln^{3+} complexes is a key property that in some cases leads to single-molecule-magnet behavior.[23] Thus, understanding the factors that control the magnetic anisotropies of mononuclear

Ln^{3+} complexes is important not only for the rational prediction of the paramagnetic NMR shifts induced by these metal ions but also in the field of molecular magnetism.[24]

Recently, we have shown that the macrocyclic ligand L^1 (Chart 1) forms very inert complexes with the Ln^{3+} ions, while a detailed study of the structure in the solid state revealed 10-coordination of the metal ions by the ligand across the whole lanthanide series from lanthanum to lutetium.[25] Furthermore, the intensity of the ^{1}H NMR signal of bulk water can be modulated by saturation of the signals of the hydroxyl protons of Pr^{3+}, Eu^{3+}, and Yb^{3+} complexes following CEST mechanisms.[25] Herein, the validity of Bleaney's theory is assessed by analyzing the ^{1}H NMR spectra of the whole series of paramagnetic Ln^{3+} ions from Ce^{3+} to Yb^{3+} (except Pm^{3+} and Gd^{3+}). The $[LnL^1]^{3+}$ complexes represent ideal candidates for this purpose because (i) they provide a complete set of isostructural complexes and experimental shifts throughout the series[26] and (ii) the $[LnL^1]^{3+}$ complexes present D_2 symmetry in solution, which provides an unequivocal location of the magnetic axes.

Results

^{1}H NMR Shifts of Paramagnetic $[LnL^1]^{3+}$ Complexes

The NMR spectra of paramagnetic $[LnL^1]^{3+}$ complexes (Ln = Ce–Yb, except Pm and Gd) were recorded in a D_2O solution at 25 °C and pH 7.0. The spectra of the complexes with Pr^{3+} and Yb^{3+}were presented in a previous paper, and the observed paramagnetic shifts were analyzed assuming a pseudocontact model.[25] All ^{1}H NMR spectra present 10 signals, which points to a D_2 symmetry of the complexes in solution, as observed previously for the Pr^{3+}, Eu^{3+}, and Yb^{3+}analogues. The representative spectra of the Dy^{3+} and Ho^{3+} complexes are presented in Figure 1, while chemical shift data of $[LnL^1]^{3+}$ complexes are provided in Table 1. A full attribution of the ^{1}H NMR signals for each $[LnL^1]^{3+}$ complex could be achieved: (i) by comparison to the assignments made to the Yb^{3+} and Pr^{3+} complexes; (ii) on the basis of the cross-peaks observed in the COSY spectra of Ce^{3+}, Pr^{3+}, Nd^{3+}, Sm^{3+}, Eu^{3+}, and Yb^{3+} complexes (see the Supporting Information); (iii) by using line-width analysis because the paramagnetic contribution to the observed line widths is proportional to $1/r^6$, where r represents the distance between the observed nucleus and the paramagnetic Ln^{3+} ion.[27] This allowed a straightforward assignment of the signals due to protons H5ax, which show particularly short Ln···H distances [3.46–3.49 Å according to our density functional theory (DFT) calculations]. Line-width analysis also allowed one to identify axial and equatorial protons because the former are generally closer to the Ln^{3+} ion, with the noticeable exception of the H6ax and H6eq protons, which present very similar Ln···H distances and thus line widths.

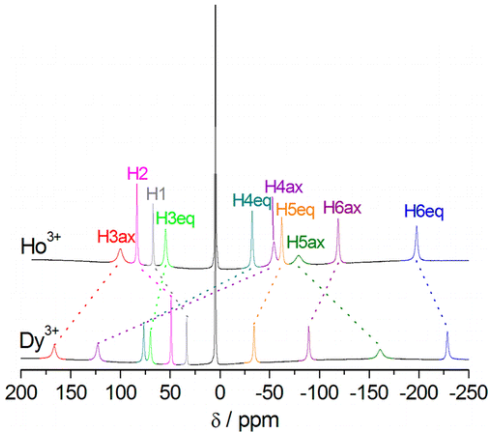

Figure 1. ^{1}H NMR spectra of the $[LnL^1]^{3+}$ complexes (Ln = Dy, Ho) recorded in a D_2O solution at 25 °C (pH 7.0, 400 MHz).

Table 1. ^{1}H NMR Shifts (D_2O, 25 °C, pH 7.0, 400 MHz) Observed for $[LnL^1]^{3+}$Complexes

	H1	H2	H3ax	H3eq	H4ax	H4eq	H5ax	H5eq	H6ax	H6eq
Ce	8.50	8.32	14.17	9.63	16.30	13.99	–8.80	2.68	3.24	–8.17
Pr[a]	9.35	10.26	22.88	16.60	25.97	25.97	–18.12	5.43	1.12	–19.90
Nd	14.62	16.17	15.14	16.17	1.06	12.08	–7.56	1.86	–4.22	–18.80
Sm	8.41	8.14	7.36	4.82	4.92	2.90	0.50	–0.27	2.25	1.54
Eu	1.45	–2.18	–12.00	–17.43	–1.85	–21.20	18.74	–3.51	10.59	33.58
Tb	14.95	25.51	148.35	48.10	148.35	78.30	–146.97	–25.32	–61.00	–178.49
Dy	33.48	49.06	166.72	70.00	122.98	76.64	–161.06	–34.18	–89.19	–228.64
Ho	67.30	83.46	100.29	54.68	–54.20	–32.39	–79.09	–62.02	–118.82	–197.78
Er	52.00	57.74	–6.40	3.50	–138.40	–95.84	32.51	–44.60	–44.60	–64.28
Tm	–9.25	–18.65	–83.39	–54.96	–53.52	–49.12	92.57	14.46	49.28	139.15
Yb[a]	–4.69	–9.43	–33.84	–19.77	–9.05	–12.79	41.87	14.11	31.65	70.34
$A/\hbar$ (rad s^{-1})	–0.0407	–0.02413	0.08105	–0.4136	0.00898	–0.6622	0.02111	–0.31956	–0.23895	0.10260

[a]Data taken from ref 25. HFCCs calculated for $[GdL^1]^{3+}$ at the DKH2/Neese/EPR-III level.

Assessment of the Contact Contributions

The contact shift caused by a Ln^{3+} ion *j* in a nucleus *i* (δ_{ij}^{con}) arises from through-bond transmission of an unpaired electron-spin density from the metal ion to the observed nucleus and can be approximated by eq 5:[14]

$$\delta_{ij}^{\mathrm{con}} = \langle S_z \rangle_j \frac{\mu_B}{3kT\gamma_I} \frac{A}{\hbar} \times 10^6 \qquad (5)$$

where $\langle S_z \rangle_j$ represents the reduced value of the average spin polarization, μ_B is the Bohr magneton, *k* is the Boltzmann constant, γ_I is the gyromagnetic ratio of the observed nucleus, $A/\hbar$ is the hyperfine coupling constant (HFCC, in rad·s^{-1}), and δ_{ij}^{con} is expressed in ppm. The values of $\langle S_z \rangle_j$ calculated for the different Ln^{3+} ions[28] are given in Table 2, together with the Bleaney factors C_j.[29] Inspection of eqs 3 and 5 shows that the relative weight of contact and pseudocontact contributions for a given Ln^{3+} ion should follow the $\langle S_z \rangle_j / C_j$ ratio. Thus, good fits according to the pseudocontact model are expected for Yb^{3+}, Tm^{3+}, Ce^{3+}, or Dy^{3+}, which present $\langle S_z \rangle_j / C_j$ ratios <0.3. On the contrary, poor fits can be anticipated for Nd^{3+} and Eu^{3+}.[30]

The δ_{ij}^{para} values of $[LnL^1]^{3+}$ complexes were estimated by using the ^{1}H NMR chemical shifts of the diamagnetic Lu^{3+} complex as a reference. The paramagnetic shifts were then initially analyzed according to a pseudocontact model with eq 2. As structural models, we have used optimized geometries obtained with DFT calculations performed in aqueous solution at the TPSSh/LCRECP/6-31G(d,p) level (Figure 2; see the computational details below). According to our calculations, the Ln–donor distances decrease across the lanthanide series following a quadratic trend, as expected for an isostructural series of Ln^{3+} complexes

(Figures S15 and S16, Supporting Information).[31,32] The quality of the agreement between the experimental and calculated shifts was assessed by using the AF_j factor defined as[33]

$$AF_j = \left[\sum_i \left(\delta_i^{exp} - \delta_i^{cal}\right)^2 / \sum_i \left(\delta_i^{exp}\right)^2\right]^{1/2} \quad (6)$$

where δ_i^{exp} represent the pseudocontact shifts obtained from the observed δ_{ij}^{para} values by subtracting the contact contribution, while δ_i^{cal} represent the pseudocontact shifts calculated with eq 2. This analysis was found in our previous paper to provide a satisfactory agreement, neglecting contact contributions for Yb^{3+} (AF_j = 0.044), while for Pr^{3+}, the agreement factor was considerably higher (AF_j = 0.112). The data presented in Table 2 show that the best agreement according to the pseudocontact model is provided by Ln^{3+} with high $C_j/\langle S_z\rangle_j$ ratios, while unacceptable AF_j values are obtained for Nd^{3+} and Eu^{3+}. These results clearly show that contact shifts provide important contributions to the overall paramagnetic shifts observed for several $[LnL^1]^{3+}$ complexes.

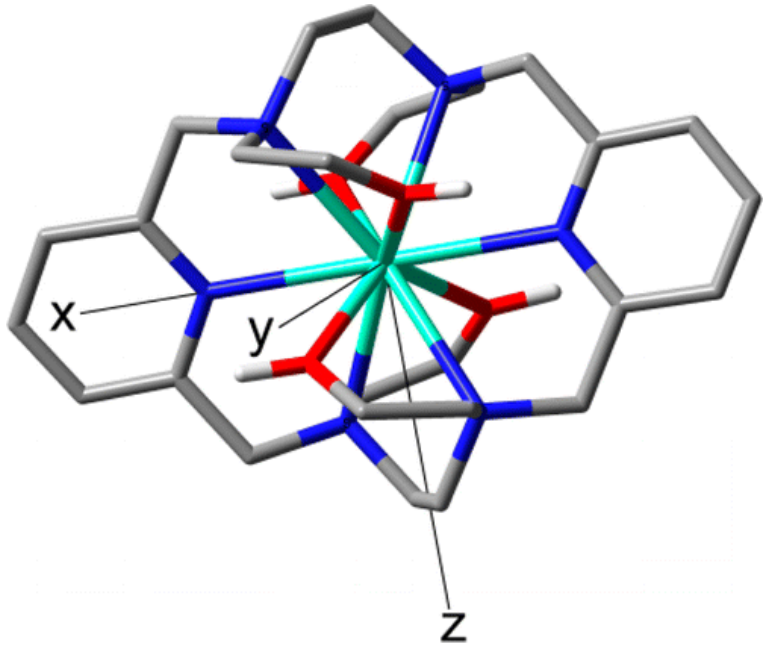

Figure 2. Structure of the $[EuL^1]^{3+}$ complex optimized in aqueous solution at the TPSSh/LCRECP/6-31G(d,p) level and orientation of the magnetic axes used in analysis of the pseudocontact shifts. H atoms, except those of hydroxyl protons, have been omitted for simplicity.

The isotropic HFCCs $A/\hbar$ responsible for the contact shifts in Ln^{3+} complexes (eq 5) are the result of the Fermi contact interaction and depend on the difference between the majority spin (α) and minority spin (β) densities at the position of the nucleus i [$\rho^{\alpha-\beta}(R_i)$] as expressed in eq 7:[34]

$$\frac{A}{\hbar} = \frac{8\pi^2}{3S}\beta_e\beta_N g_e g_N \rho^{\alpha-\beta}(R_i) \quad (7)$$

where β_N and β_e are the nuclear and Bohr magnetons, respectively, g_N and g_e are the nuclear and free-electron g values, and S is the total electron spin of the system. In a previous work, we have shown that all-electron relativistic DFT calculations based on the second-order Douglas–Kroll–Hess (DKH2) method (DKH2/Neese/EPR-III) provide accurate $A/\hbar$ values for different Gd^{3+}complexes.[35,36] Similar calculations performed for $[GdL^1]^{3+}$ provide the HFCCs listed in Table 1. The calculated $A/\hbar$ values present different signs depending on the nucleus under consideration, which shows that the spin-density distribution is dominated by the spin-polarization mechanism, which is the result of an effective attraction of unpaired electrons to the nearby ones of the same spin.[37] The proton nuclei of the pyridyl units H1 and H2 present very low calculated $A/\hbar$ values because they are rather far away from the metal center in terms of the number of bonds. Important negative $A/\hbar$ values are calculated for the equatorial protons of the ligands H3–H6, while the axial protons present positive HFCCs with smaller absolute values. These results are in line with our previous calculations, which showed that the $A/\hbar$ values are very sensitive to the H–C–X–Gd dihedral angle (X = N or O).[36]

Table 2. Values of C_j at Room Temperature, Values of $\langle S_z \rangle$ and Effective $\langle S_z \rangle$ ($\langle S_z \rangle^{eff}$) Values, Axial ($\Delta\chi_{ax}$) and Rhombic ($\Delta\chi_{rh}$) Magnetic Susceptibilities, and Agreement Factors (AF_j) Obtained from Analysis of the Paramagnetic ^{1}H NMR Shifts of $[LnL^1]^{3+}$ Complexes

	C_j [a]	$\langle S_z \rangle$ [b]	$\langle S_z \rangle^{eff}$ [c]	$\Delta\chi_{ax} \times 10^{-32}$ m^3 [d]	$\Delta\chi_{rh} \times 10^{-32}$ m^3 [d]	AF_j [e]	AF_j [f]
Ce	–6.3	–0.974	–0.037	–1.97 ± 0.05	–1.68 ± 0.08	0.0770	0.0770
Pr	–11.0	–2.956	–2.370	–3.59 ± 0.02	–2.76 ± 0.05	0.1115	0.0452
Nd	–4.2	–4.452	–3.577	–0.32 ± 0.03	–4.21 ± 0.04	0.2415	0.0507
Sm	–0.7	0.06	[g]	[g]	[g]	[g]	[g]
Eu	4.0	10.68	10.06	1.20 ± 0.04	4.75 ± 0.06	0.4370	0.0577
Tb	–86	31.853	22.01	–22.5 ± 0.2	–23.1 ± 0.3	0.1505	0.0418
Dy	–100	28.565	15.88	–20.1 ± 0.2	–33.2 ± 0.3	0.1013	0.0335
Ho	–39	22.642	11.44	3.1 ± 0.2	–39.7 ± 0.3	0.0940	0.0429
Er	33	15.382	6.079	17.3 ± 0.2	–18.3 ± 0.3	0.0988	0.0732
Tm	53	8.210	4.710	9.6 ± 0.2	19.5 ± 0.2	0.0697	0.0500
Yb	22	2.589	1.371	2.74 ± 0.05	10.57 ± 0.07	0.0449	0.0321

[a]Values at 300 K scaled to −100 for Dy taken from ref 29. [b]From ref 28. [c]Effective $\langle S_z \rangle$ values obtained from analysis of the paramagnetic shifts (see the text). [d]Axis orientations are defined according to Figure 2. [e]Neglecting contact contributions. [f]Including contact contributions. [g]Sm^{3+} was not included in the analysis because of the small paramagnetic shifts induced by this ion.

Analysis of the ^{1}H NMR Paramagnetic Shifts Including Contact Contributions

The $A/\hbar$ values obtained with the aid of DFT calculations can be used to estimate the contact contributions of each ligand nuclei with eq 5 and the $\langle S_z \rangle$ values available in the literature.[28] This approach was successfully applied to analyze the paramagnetic ^{1}H NMR shifts of different Tb^{3+}complexes, including $[TbL^2]^-$ and $[TbL^3]^{3+}$ (Chart 1).[36] Subsequently, the pseudocontact contributions can be obtained by subtracting the contact contributions from the overall paramagnetic shifts (eq 1). In the case of $[TbL^2]^-$, the pseudocontact shifts obtained by using this methodology were found to be in good agreement with those obtained by

Berardozzi and Di Bari using a completely different approach.[38] Our initial analysis of the paramagnetic shifts observed for $[TbL^1]^{3+}$ afforded similar results because the agreement factor improved noticeably upon the inclusion of contact shifts. However, this preliminary analysis also showed that the use of $\langle S_z \rangle$ values somewhat different from those reported in the literature resulted in better agreement factors. This is illustrated for the representative $[PrL^1]^{3+}$ and $[DyL^1]^{3+}$ complexes in Figure 3. Thus, for each $[LnL^1]^{3+}$ complex, the paramagnetic shifts were analyzed by varying $\langle S_z \rangle$ around the tabulated values and calculating the agreement factors AF_j at each point. The plots of AF_j versus $\langle S_z \rangle$ were subsequently fitted to a fourth-degree polynomial function, which presents a minimum that provides an effective $\langle S_z \rangle$ value ($\langle S_z \rangle^{eff}$), giving the best agreement between the experimental and calculated paramagnetic ^{1}H NMR shifts (Table 2). An important improvement of the agreement factors was observed for all Ln^{3+} ions upon the inclusion of contact contributions, with the exception of Ce^{3+}, which provided an $\langle S_z \rangle^{eff}$ value very close to zero (Table 2). The agreement factors obtained upon the inclusion of contact contributions are very good, ranging from 0.032 for Yb^{3+} to 0.077 for Ce^{3+}. Obviously, a particularly important improvement of the agreement between the experimental and calculated paramagnetic shifts is observed for those complexes with important contact shifts such as $[EuL^1]^{3+}$. This becomes evident by comparing the absolute differences between the experimental and calculated paramagnetic shifts ($\Delta\delta$) with and without the inclusion of contact shifts (Figure 4). Neglecting the contact contribution results in very large deviations of the experimental and calculated shifts (up to 13.1 ppm), noticeably in the case of equatorial protons. Considering the contact contributions in the analysis of the paramagnetic shifts reduces the $\Delta\delta$ values to 0.04–1.72 ppm.

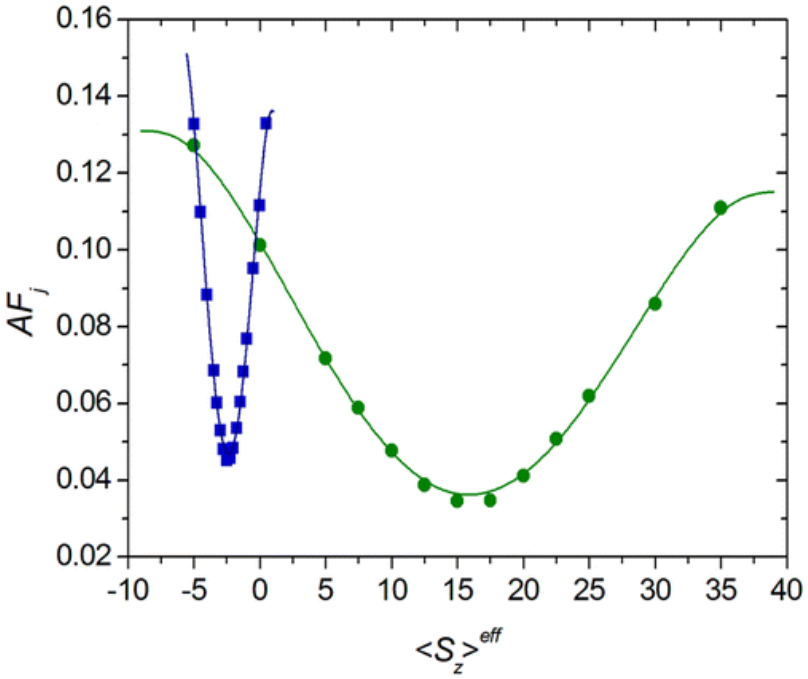

Figure 3. Plot of the agreement factor AF_j versus the effective $\langle S_z \rangle$ value used in analysis of the ^{1}H NMR paramagnetic shifts of $[PrL^1]^{3+}$ (squares) and $[DyL^1]^{3+}$ (circles). The solid lines represent the fit of the data with minima at $\langle S_z \rangle^{eff}$ of −2.37 (Pr) and 15.88 (Dy).

The calculated $\langle S_z \rangle^{eff}$ values (Table 2) deviate significantly from those reported in the literature for most of the Ln^{3+} ions. These differences could arise from the inaccuracy of the $\langle S_z \rangle$ values available in the literature, which were obtained by neglecting the ligand-field splitting of the *J* manifold,[37] but could also be the result of errors in the $A/\hbar$ values obtained with our DFT calculations, changes in the HFCCs along the lanthanide series, or a combination of these three factors. Whatever the reasons for these deviations, the $\langle S_z \rangle$ values

obtained for $[LnL^1]^{3+}$complexes and the theoretical values provide a rather good linear correlation ($R^2 > 0.98$; Figure S14, Supporting Information), which provides support to our methodology.

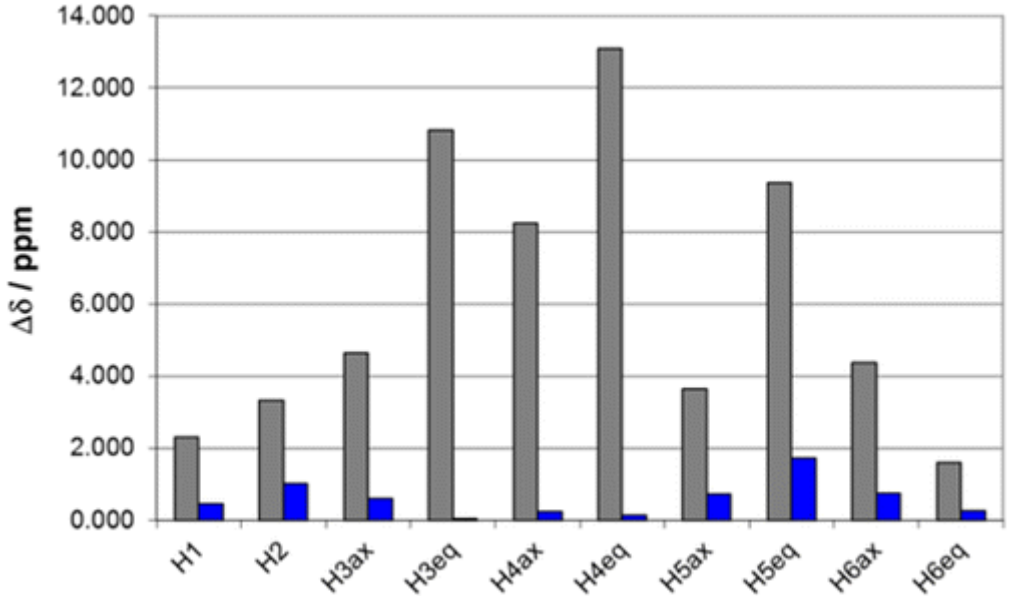

Figure 4. Absolute deviations (Δδ) of experimental and calculated Eu^{3+}-induced ^{1}H NMR shifts in $[EuL^1]^{3+}$. Color code: gray, neglecting contact contributions; blue, including contact contributions.

Analysis of the Magnetic Anisotropy

Analysis of the paramagnetic ^{1}H NMR shifts of $[LnL^1]^{3+}$ complexes provides axial ($\Delta\chi_{ax}$) and rhombic ($\Delta\chi_{rh}$) anisotropies of the magnetic susceptibility tensor. Assuming that the magnetic axes coincide with the three C_2 symmetry axes of the molecule, analysis of the pseudocontact shifts according to eq 2 still yields six degenerate solutions that correspond to the six different orientations of the magnetic axes. For each of these solutions, the calculated shifts (and thus agreement factors AF_j) are identical, but the values of $\Delta\chi_{ax}$ and $\Delta\chi_{rh}$ are different. Thus, we have taken the arbitrary orientation of the principal axes of the magnetic susceptibility tensor shown in Figure 2, which provides the $\Delta\chi_{ax}$ and $\Delta\chi_{rh}$ values listed in Table 2.

The magnetic anisotropies calculated for $[LnL^1]^{3+}$ complexes follow the qualitative trends predicted by Bleaney's theory for most of the lanthanide ions, with the noticeable exceptions of Ho^{3+} and Er^{3+}. Indeed, the C_j value reported for Ho^{3+} (−39) has the same sign as those of Tb^{3+}(−86) and Dy^{3+} (−100), and therefore the $\Delta\chi_{ax}$ and $\Delta\chi_{rh}$ values characterizing the magnetic anisotropies of these complexes should have identical signs. However, this is not the case. This anomalous behavior can already be noticed by a simple inspection of the spectra shown in Figure 1. Indeed, according to Bleaney's constants, the paramagnetic shifts of the Ho^{3+} complex should amount to about 39% of those observed for the Dy^{3+} analogue. However, certain proton signals observed for $[HoL^1]^{3+}$ present larger shifts compared with $[DyL^1]^{3+}$ (i.e., H1 and H2, which can be unequivocally assigned on the basis of their integration and line widths), and furthermore the signs of some of the resonances are reversed. A comparison of the spectra recorded for the Er^{3+}, Tm^{3+}, and Yb^{3+} complexes also reveals the anomalous behavior of the Er^{3+} complex. Plots of Bleaney's factors versus the $\Delta\chi_{ax}$ and $\Delta\chi_{rh}$ values provide reasonably good linear correlations when $Ho^{3+}$and Er^{3+} are excluded from the fit (Figure 5) but clearly highlight that the latter two metal ions do not follow the trend expected according to Bleaney's theory.

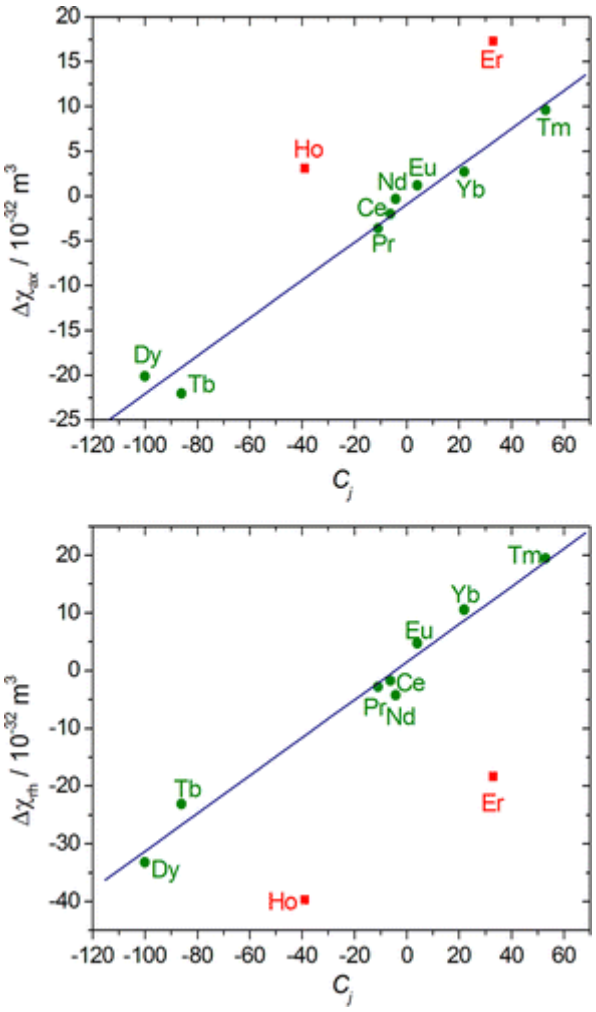

Figure 5. Plots of Bleaney's factors C_j versus the $\Delta\chi_{ax}$ and $\Delta\chi_{rh}$ values obtained for $[LnL^1]^{3+}$ complexes. The solid lines correspond to linear fits of the data ($R^2 > 0.988$) excluding Ho^{3+} and Er^{3+}.

Discussion and Conclusions

The present contribution has shown that the paramagnetic ^{1}H NMR shifts of $[LnL^1]^{3+}$ complexes do not follow the trend expected according to Bleaney's factors. The validity of this theory has been the subject of debate during the last 15 years. In particular, Bleaney assumed that the ligand-field splitting is smaller than *kT*, so that the crystal-field levels of the ground multiplet should have comparable populations at room temperature. The assumption was questioned by Binnemans and co-workers using numerical simulations of the magnetic anisotropies of lanthanide complexes considering different coordination numbers and coordination polyhedra.[19] These simulations predicted that for most coordination polyhedra the signs of the magnetic anisotropy should follow the trends predicted by Bleaney, with the noticeable exceptions of coordination polyhedra in which rank-two crystal-field parameters are small or zero. In such cases, the sign of the magnetic anisotropy could be irregular. The results obtained in this study provide experimental evidence for the behavior predicted by Binnemans and co-workers, and later suggested by Parker and co-workers from analysis of the shifts observed for pyridyl protons located at least four bonds away from the metal ion (Ln = Tb–Yb).[21]

The study presented in this paper allowed us to calculate a reliable set of magnetic anisotropies for all paramagnetic rhombic $[LnL^1]^{3+}$ complexes (except Pm and Gd), which required an accurate estimation of the contact contributions to the paramagnetic shifts. This was achieved in the past by using the Reilley

method,[39] which allows the separation of contact and pseudocontact contributions relying on several assumptions: (i) A series of complexes is isostructural along the lanthanide series. (ii) The Bleaney constants C_j and spin expectation values $\langle S_z \rangle$ do not differ significantly from the tabulated values. (iii) The crystal-field parameters and HFCCs do not change across the lanthanide series. The Reilley method was, however, shown to perform poorly for complexes that did not show important structural changes across the series, such as, for instance, the $[LnL^2]^-$ and $[Ln(DPA)]^{3-}$ (DPA = 2,6-dipicolinate) derivatives.[40,41] Another notable example was provided recently with analysis of the magnetic anisotropy in endohedral nitride clusterfullerenes, which revealed remarkable deviations from the linear trends expected according to the Reilley method for Tb^{3+} and Tm^{3+}.[42] Application of the Reilley method to the $[LnL^1]^{3+}$complexes results in plots of $\delta_{ij}^{para}/\langle S_z \rangle_j$ versus $C_j/\langle S_z \rangle_j$ that are clearly nonlinear, confirming that the conditions mentioned above are not fulfilled (Figure S17, Supporting Information).

The methodology reported here does not rely on any of the assumptions listed above, and it only requires a reasonable estimate of the relative values of the HFCCs for the different Ln^{3+}complexes from DFT calculations performed on the Gd^{3+} analogue.[36] Even in the case that the $A/\hbar$ values change considerably across the series, the plots such as those in Figure 3 correct these deviations if the relative values for the different nuclei do not change significantly.

A full set of magnetic anisotropies was reported by Bertini et al. for the Ln^{3+} ions fixed in a protein matrix.[22] This approach avoids any contamination of the paramagnetic shifts with contact contributions, which are expected to be important only for nuclei placed a few bonds away from the paramagnetic center. Bertini et al. concluded in that study that the magnetic anisotropies followed reasonably well the predictions of Bleaney's theory. In view of the results reported here, it is clear that, in spite of its usefulness to rationalize the paramagnetic shifts of many series of Ln^{3+}complexes, Bleaney's theory should be used with care because it might fail even in making qualitative predictions.

The paramagnetic shifts induced by the Ln^{3+} ions have been used for different applications for more than 40 years. However, some recent studies have witnessed that subtle changes in the Ln^{3+} coordination environment may provoke drastic changes in the magnetic anisotropies of these ions. For instance, it has been shown that the formation of fluoride dimers with linear Ln–F–Ln bridging units caused dramatic changes in the observed ^1H NMR shifts induced by Yb^{3+},[43] while the binding of F^- to Ln^{3+}(DOTA) tetraamide complexes provoked a change of the magnetic anisotropy from a prolate to an oblate distribution or vice versa.[44] The results reported here represent a significant advance for rationalization of the paramagnetic shifts induced by the Ln^{3+}ions, with a great potential impact for the development of PARASHIFT contrast agents[21] and the application of paramagnetic Ln^{3+} ions in NMR spectroscopy of proteins.[45]

Experimental and Computational Section

NMR Spectroscopy

^1H NMR spectra were recorded at 25 °C in solutions of the complexes in D_2O on a Bruker ARX400 spectrometer. Chemical shifts were referenced by using the residual solvent proton signal (δ = 4.79 ppm).[46]

Computational Details

All calculations presented in this work were performed by employing the *Gaussian 09* package (revision D.01).[47] As for the Pr and Yb complexes reported in our previous work, full geometry optimizations of the $[LnL^1]^{3+}$ systems (Ln = Ce, Nd, Eu, Gd, Tb, Ho, Er, Tm) were performed in aqueous solution employing DFT within the hybrid meta generalized gradient approximation, with the TPSSh exchange-correlation

functional.[48] The large-core quasirelativistic effective core potentials (ECPs) and associated [5s4p3d]-GTO basis sets of Dolg and co-workers were used for the lanthanides,[49] while the ligand atoms were described using the standard 6-31G(d,p) basis set. The stationary points found on the potential energy surfaces as a result of the geometry optimizations have been tested to represent true energy minima using frequency analysis. HFCCs of the ligand nuclei in $[GdL^1]^{3+}$ were computed using the all-electron DKH2 method, as implemented in *Gaussian 09*,[50] with the all-electron scalar relativistic basis set of Pantazis and Neese for the Gd atom[51] and the EPR-III basis sets of Barone for C, H, N, and O atoms.[52] EPR-III is a triple-ζ basis set optimized for the computation of HFCCs that includes diffuse functions, double d polarizations, a single set of f-polarization functions, and an improved s part to better describe the nuclear region. Bulk water solvent effects were included by using the polarizable continuum model, in which the solute cavity is built as an envelope of spheres centered on atoms or atomic groups with appropriate radii. In particular, we used the integral equation formalism[53] variant, as implemented in *Gaussian 09*. The universal-force-field[54] radii scaled by a factor of 1.1 were used to define the solute cavity.

Associated Content

Supporting Information

The Supporting Information is available free of charge on the ACS Publications website at DOI: 10.1021/acs.inorgchem.5b02918.

- ^{1}H and ^{1}H–^{1}H COSY NMR spectra, experimental and calculated paramagnetic shifts and contact and pseudocontact contributions, bond distances and optimized geometries obtained with DFT, plots of $\langle S_z \rangle^{eff}$ versus $\langle S_z \rangle$ and $\langle S_z \rangle^{eff}$ versus AF_j, and complete ref 45 (PDF)

Author Information

Corresponding Author

*E-mail: carlos.platas.iglesias@udc.es.

Author Contributions

The manuscript was written through contributions of all authors. All authors have given approval to the final version of the manuscript.

Notes

The authors declare no competing financial interest.

Acknowledgment

M.R.-F., D.E.-G., and C.P.-I. thank the Ministerio de Economía y Competitividad (Grant CTQ2013-43243-P) for generous financial support. L.V. and P.P.-L. thank the Ministerio de Ciencia e Innovación, Plan Nacional de I+D+i (Grant CTQ2011-24487) for financial support. The authors are indebted to Centro de Supercomputación of Galicia for providing the computer facilities.

References

(1) (a) Horrocks, W. DeW., Jr.; Sipe, J. P., III *J. Am. Chem. Soc.* **1971**, 93, 6800−6804. (b) Hinckley, C. C. *J. Am. Chem. Soc.* **1969**, 91, 5160−5162.

(2) Geraldes, C. F. G. C. Lanthanide Shift Reagents. In *The Rare Earth Elements: Fundamentals and Applications*; Atwood, D. A., Ed.; Wiley: Chichester, U.K., 2012. pp 501−520.

(3) (a) Wenzel, T. J.; Wilcox, J. D. *Chirality* **2003**, 15, 256−270. (b) Aspinall, H. C. *Chem. Rev.* **2002**, 102, 1807−1850. (c) Ghosh, I.; Zeng, H.; Kishi, Y. *Org. Lett.* **2004**, 6, 4715−4718.

(4) (a) Gencic, M. S.; Radulovic, N. S. *RSC Adv.* **2015**, 5, 72670−72682. (b) Rachineni, K.; Kakita, V. M. R.; Dayaka, S.; Vemulapalli, S. P. B.; Bharatam, J. *Anal. Chem.* **2015**, 87, 7258−7266.

(5) (a) Yamaguchi, T.; Sakae, Y.; Zhang, Y.; Yamamoto, S.; Okamoto, Y.; Kato, K. *Angew. Chem., Int. Ed.* **2014**, 53, 10941−10944. (b) Barry, C. D.; North, A. C. T.; Glasel, J. A.; Williams, R. J. P.; Xavier, A. V. *Nature* **1971**, 232, 236−245.

(6) (a) Keizers, P. H. J.; Mersinli, B.; Reinle, W.; Donauer, J.; Hiruma, Y.; Hannemann, F.; Overhand, M.; Bernhardt, R.; Ubbink, M. *Biochemistry* **2010**, 49, 6846−6855. (b) Su, X. C.; Liang, H.; Loscha, K. V.; Otting, G. *J. Am. Chem. Soc.* **2009**, 131, 10352−10353. (c) John, M.; Pintacuda, G.; Park, A. Y.; Dixon, N. E.; Otting, G. *J. Am. Chem. Soc.* **2006**, 128, 12910−12916.

(7) (a) Puckeridge, M.; Chapman, B. E.; Conigrave, A. D.; Kuchel, P. W. *J. Inorg. Biochem.* **2012**, 115, 211−219. (b) Buster, D. C.; Castro, M. C. A.; Geraldes, C. F. G. C.; Malloy, C. R.; Sherry, A. D.; Siemers, T. C. *Magn. Reson. Med.* **1990**, 15, 25−32.

(8) *The Chemistry of Contrast Agents in Medical Magnetic Resonance Imaging*, 2nd ed.; Merbach, A. E., Helm, L., Tóth, E., Eds.; Wiley: New York, 2013.

(9) (a) Aime, S.; Crich, S. G.; Gianolio, E.; Giovenzana, G. B.; Tei, L.; Terreno, E. *Coord. Chem. Rev.* **2006**, 250, 1562−1579. (b) Terreno, E.; Castelli, D. D.; Aime, S. *Contrast Media Mol. Imaging* **2010**, 5, 78−98.

(10) (a) Ratnakar, S. J.; Woods, M.; Lubag, A. J. M.; Kovacs, Z.; Sherry, A. D. *J. Am. Chem. Soc.* **2008**, 130, 6−7. (b) Ratnakar, S. J.; Soesbe, T. C.; Lumata, L. L.; Do, Q. N.; Viswanathan, S.; Lin, C.-Y.; Sherry, A. D.; Kovacs, Z. *J. Am. Chem. Soc.* **2013**, 135, 14904−14907. (c) Zhang, S.; Michaudet, L.; Burgess, S.; Sherry, A. D. *Angew. Chem., Int. Ed.* **2002**, 41, 1919−1921. (d) Viswanathan, S.; Ratnakar, S. J.; Green, K. N.; Kovacs, Z.; De Leon-Rodriguez, L. M.; Sherry, A. D. *Angew. Chem., Int. Ed.* **2009**, 48, 9330−9333. (e) Chauvin, T.; Durand, P.; Bernier, M.; Meudal, H.; Doan, B.-T.; Noury, F.; Badet, B.; Beloeil, J.-C.; Toth, E. *Angew. Chem., Int. Ed.* **2008**, 47, 4370−4372. (f) Liu, G.; Li, Y.; Pagel, M. D. *Magn. Reson. Med.* **2007**, 58, 1249−1256. (g) Zhang, S.; Winter, P.; Wu, K.; Sherry, A. D. *J. Am. Chem. Soc.* **2001**, 123, 1517−1518. (h) Huang, Y.; Coman, D.; Ali, M. M.; Hyder, F. *Contrast Media Mol. Imaging* **2015**, 10, 51−58. (i) Zhang, S.; Merritt, M.; Woessner, D. E.; Lenkinski, R. E.; Sherry, A. D. *Acc. Chem. Res.* **2003**, 36, 783−790. (j) Green, K. N.; Viswanathan, S.; Rojas-Quijano, F. A.; Kovacs, Z.; Sherry, A. D. *Inorg. Chem.* **2011**, 50, 1648−1655. (k) Zhang, S.; Wu, K.; Biewer, M. C.; Sherry, A. D. *Inorg. Chem.* **2001**, 40, 4284−4290.

(11) (a) Aime, S.; Delli Castelli, D.; Terreno, E. *Angew. Chem., Int. Ed.* **2005**, 44, 5513−5515. (b) Ferrauto, G.; Di Gregorio, E.; Baroni, S.; Aime, S. *Nano Lett.* **2014**, 14, 6857−6862.

(12) Harvey, P.; Blamire, A. M.; Wilson, J. I.; Finney, K.-L. N. A.; Funk, A. M.; Senanayake, P. K.; Parker. *Chem. Sci.* **2013**, 4, 4251−4258.

(13) Forsberg, J. H.; Delaney, R. M.; Zhao, Q.; Harakas, G.; Chandran, R. *Inorg. Chem.* **1995**, 34, 3705−3715.

(14) (a) Peters, J. A.; Huskens, J.; Raber, D. J. *Prog. Nucl. Magn. Reson. Spectrosc.* **1996**, 28, 283−350. (b) Bertini, I.; Luchinat, C.; Parigi, G. *Prog. Nucl. Magn. Reson. Spectrosc.* **2002**, 40, 249−273.

(15) Bleaney, B. *J. Magn. Reson.* **1972**, 8, 91−100.

(16) Terazzi, E.; Rivera, J.-P.; Ouali, N.; Piguet, C. *Magn. Reson. Chem.* **2006**, 44, 539−552.

(17) Piguet, C.; Geraldes, C. Paramagnetic NMR Lanthanide Induced Shifts for Extracting Solution Structures. In *Handbook on the Physics and Chemistry of Rare Earths*; Gschneidner, K. A., Bunzli, J.-C., Pecharsky, V., Eds.; Elsevier: Amsterdam, The Netherlands, 2003; Vol. 33; pp 353−463.

(18) (a) Ren, J.; Sherry, A.- D. *J. Magn. Reson., Ser. B* **1996**, 111, 178−182. (b) Platas, C.; Avecilla, F.; de Blas, A.; Geraldes, C. F. G. C.; Rodríguez-Blas, T.; Adams, H.; Mahía, J. *Inorg. Chem.* **1999**, 38, 3190−3199. (c) Rigault, S.; Piguet, C. *J. Am. Chem. Soc.* **2000**, 122, 9304−9305. (d) Ouali, N.; Rivera, J.-P.; Chapon, D.; Delangle, P.; Piguet, C. *Inorg. Chem.* **2004**, 43, 1517−1529.

(19) Mironov, V. S.; Galyametdinov, Y. G.; Ceulemans, A.; Görller-Walrand, C.; Binnemans, K. *J. Chem. Phys.* **2002**, 116, 4673−4685.

(20) Charnock, G. T. P.; Kuprov, I. *Phys. Chem. Chem. Phys.* **2014**, 16, 20184−20189.

(21) Funk, A. M.; Finney, K.-L. N. A.; Harvey, P.; Kenwright, A. M.; Neil, E. R.; Rogers, N. J.; Senanayake, P. K.; Parker, D. *Chem. Sci.* **2015**, 6, 1655−1662.

(22) Bertini, I.; Janik, M. B. L.; Lee, Y.-M.; Luchinat, C.; Rosato, A. *J. Am. Chem. Soc.* **2001**, 123, 4181−4188.

(23) (a) Zhang, P.; Jung, J.; Zhang, L.; Tang, J.; Le Guennic, B. *Inorg. Chem.* **2016**, 55, 1905−1911. (b) Gregson, M.; Chilton, N. F.; Ariciu, A.-M.; Tuna, F.; Crowe, I. F.; Lewis, W.; Blake, A. J.; Collison, D.; McInnes, E. J. L.; Winpenny, R E. P.; Liddle, S. T. *Chem. Sci.* **2016**, 7, 155−165. (c) Brown, A. J.; Pinkowicz, D.; Saber, M. R.; Dunbar, K. R. *Angew. Chem., Int. Ed.* **2015**, 54, 5864−5868. (d) Ishikawa, N.; Sugita, M.; Ishikawa, T.; Koshihara, S.-Y.; Kaizu, Y. *J. Am. Chem. Soc.* **2003**, 125, 8694−8695. (e) Cucinotta, G.; Perfetti, M.; Luzon, J.; Etienne, M.; Car, P.-E.; Caneschi, A.; Calvez, G.; Bernot, K.; Sessoli, R. *Angew. Chem., Int. Ed.* **2012**, 51, 1606−1610.

(24) Woodruff, D. N.; Winpenny, R. E. P.; Layfield, R. A. *Chem. Rev.* **2013**, 113, 5110−5148.

(25) Castro, G.; Regueiro-Figueroa, M.; Esteban-Gómez, D.; Bastida, R.; Macías, A.; Pérez-Lourido, P.; Platas-Iglesias, C.; Valencia, L. *Chem.- Eur. J.* **2015**, 21, 18662−18670.

(26) Di Pietro, S.; Piano, S. L.; Di Bari, L. *Coord. Chem. Rev.* **2011**, 255, 2810−2820.

(27) Aime, S.; Barbero, L.; Botta, M.; Ermondi, G. *J. Chem. Soc., Dalton Trans.* **1992**, 225−228.

(28) Pinkerton, A. A.; Rossier, M.; Spiliadis, S. *J. Magn. Reson.* **1985**, 64, 420−425.

(29) Golding, R. M.; Pyykkö, P. *Mol. Phys.* **1973**, 26, 1389−1396.

(30) Lisowski, J.; Sessler, J. L.; Lynch, V.; Mody, T. D. *J. Am. Chem. Soc.* **1995**, 117, 2273−2285.

(31) Seitz, M.; Oliver, A. G.; Raymond, K. N. *J. Am. Chem. Soc.* **2007**, 129, 11153−11160.

(32) Regueiro-Figueroa, M.; Esteban-Gómez, D.; de Blas, A.; Rodríguez-Blas, T.; Platas-Iglesias, C. *Chem. - Eur. J.* **2014**, 20, 3974−3981.

(33) (a) Willcott, M. R.; Lenkinski, R. E.; Davis, R. E. *J. Am. Chem. Soc.* **1972**, 94, 1742−1744. (b) Davis, R. E.; Willcott, M. R. J. *Am. Chem. Soc.* **1972**, 94, 1744−1745.

(34) Neese, F. *Coord. Chem. Rev.* **2009**, 253, 526−563.

(35) Esteban-Gomez, D.; de Blas, A.; Rodriguez-Blas, T.; Helm, L.; Platas-Iglesias, C. *ChemPhysChem* **2012**, 13, 3640−3650.

(36) Rodriguez-Rodriguez, A.; Esteban-Gomez, D.; de Blas, A.; Rodriguez-Blas, T.; Botta, M.; Tripier, R.; Platas-Iglesias, C. *Inorg. Chem.* **2012**, 51, 13419−13429.

(37) Bertini, I.; Luchinat, C. *Coord. Chem. Rev.* **1996**, 150, 29−75.

(38) Berardozzi, R.; Di Bari, L. *Inorg. Chem.* **2013**, 52, 11514−11518.

(39) Reilley, C. N.; Good, B. W.; Desreux, J. F. *Anal. Chem.* **1975**, 47, 2110−2116.

(40) Valencia, L.; Martínez, J.; Macías, A.; Bastida, R.; Carvalho, R. A.; Geraldes, C. F. G. C. *Inorg. Chem.* **2002**, 41, 5300−5312.

(41) Ouali, N.; Bocquet, B.; Rigault, S.; Morgantini, P.-Y.; Weber, J.; Piguet, C. *Inorg. Chem.* **2002**, 41, 1436−1445.

(42) Zhang, Y.; Krylov, D.; Rosenkranz, M.; Schiemenz, S.; Popov, A. A. *Chem. Sci.* **2015**, 6, 2328−2341.

(43) Liu, T.; Nonat, A.; Beyler, M.; Regueiro-Figueroa, M.; Nchimi Nono, K.; Jeannin, O.; Camerel, F.; Debaene, F.; Cianférani-Sanglier, S.; Tripier, R.; Platas-Iglesias, C.; Charbonnière, L. J. *Angew. Chem., Int. Ed.* **2014**, 53, 7259−7263.

(44) (a) Blackburn, O. A.; Chilton, N. F.; Keller, K.; Tait, C. E.; Myers, W. K.; McInnes, E. J. L.; Kenwright, A. M.; Beer, P. D.; Timmel, C. R.; Faulkner, S. *Angew. Chem., Int. Ed.* **2015**, 54, 10783−10786. (b) Blackburn, O. A.; Kenwright, A. M.; Beer, P. D.; Faulkner, S. *Dalton Trans.* **2015**, 44, 19509−19517.

(45) Liu, W.-M.; Overhand, M.; Ubbink, M. *Coord. Chem. Rev.* **2014**, 273−273, 2−12.

(46) Fulmer, G. R.; Miller, A. J. M.; Sherden, N. H.; Gottlieb, H. E.; Nudelman, A.; Stoltz, B. M.; Bercaw, J. E.; Goldberg, K. I. *Organometallics* **2010**, 29, 2176−2179.

(47) Frisch, M. J. *Gaussian 09*, revision D.01; Gaussian, Inc.: Wallingford, CT, 2010.

(48) Tao, J. M.; Perdew, J. P.; Staroverov, V. N.; Scuseria, G. E. *Phys. Rev. Lett.* **2003**, 91, 146401.

(49) Dolg, M.; Stoll, H.; Savin, A.; Preuss, H. *Theor. Chim. Acta* **1989**, 75, 173−194.

(50) (a) Barysz, M.; Sadlej, A. J. *J. Mol. Struct.: THEOCHEM* **2001**, 573, 181−200. (b) Reiher, M. *Theor. Chem. Acc.* **2006**, 116, 241−252.

(51) Pantazis, D. A.; Neese, F. *J. Chem. Theory Comput.* **2009**, 5, 2229−2238.

(52) Rega, N.; Cossi, M.; Barone, V. J. *J. Chem. Phys.* **1996**, 105, 11060−11067.

(53) Tomasi, J.; Mennucci, B.; Cammi, R. *Chem. Rev.* **2005**, 105, 2999−3093.

(54) Rappe, A. K.; Casewit, C. J.; Colwell, K. S.; Goddard, W. A., III; Skiff, W. M. *J. Am. Chem. Soc.* **1992**, 114, 10024−10035.